Noninvasive Measurement of Heart Rate and Respiratory Rate for Perioperative Infants

Yi Zhang, *Member, IEEE,* Zhihao Chen, *Senior Member, IEEE,* and Hwan Ing Hee

***Abstract*—A novel fiber optic sensor is designed with mesh microbenders for simultaneous perioperative measurement of heart rate (HR) and respiratory rate (RR) for infants. The feasibility of the mesh microbend fiber sensor was evaluated in 10 infants, ranging from 1 to 12 months in a prospective cross-sectional observational study with the sensor placed under the subjects in the perioperative period. All study subjects received standard intraoperative physiological monitoring of their vital signs. The high order harmonic sensing signals associated with other filtering methods are used for the removal of motion noise. The study results showed good agreement in the measurement of HR and RR between the proposed microbend fiber sensor and the current standard physiological monitoring used in medical settings.**

***Index Terms*—Microbend optical fiber, heart rate (HR), respiratory rate (RR), perioperative infant monitoring.**

I. Introduction

MONITORING of a patient's physiological status is a vital part of standard medical care to provide reliable and objective information about the body's basic function and health status. These vital signs are used to evaluate clinical condition, detect clinical deterioration and facilitate appropriate medical intervention. Heart rate (HR) and respiratory rate (RR) are two of the four vital signs being routinely monitored by medical professionals and health care providers. Limitations in current monitoring technology include the need for direct patient contact with the device, restriction of patient's movement by cables and sensors, single monitoring device per vital sign, interference of readings as a result of poor contact between sensors and skin. Infants, in particular, tolerate placement of multiple monitors poorly resulting in agitation and poor compliance. An ideal technology is the one that enables real-time and rapid accurate measurements while being minimally intrusive and invasive.

In recent years, there has been a rapid emergence of new technology that operates on a non-intrusive platform that neither requires cable attachment nor direct body skin contact. Those new sensors offer the patients the value-added comfort, ease of use, and freedom of activities without physical constraint. More importantly, those new sensors enable automated and simultaneous measurement of both HR and RR, including Emfit sensor [1], air mattress sensor [2], liquid pressure sensor [3], ECG sensor [4], Doppler radar sensor [5], acoustic sensor [6], and electronic weighing scale [7]. Nevertheless, they are prone to electromagnetic interference and radiofrequency (RF) heating if they are used in magnetic resonance imaging (MRI), particularly in the high-field MRI environment. The advent of optical fiber sensor provides an attractive and feasible option for clinical use in high-field MRI environment as optical fiber sensors are passive, free of electromagnetic interference, and being MRI safe. Many types of optical fiber sensors have been proposed for HR and RR monitoring, including photoplethysmography (PPG) based fiber optic sensor [8], interferometric fiber optic sensor [9, 10], fiber optic speckle sensor [11], fiber Bragg grating sensor [12–22], hetero-core fiber optic pressure sensors [23] and fiber laser sensor [24]. Interferometric fiber optic sensor has very high sensitivity but it requires a coherent light source and complex interrogation. Fiber optic speckle sensor requires the use of coherent light source and bulk optics [11]. Fiber Bragg grating sensor is a promising sensor for measurement of HR and RR. However, FBG's wavelength detection mechanism is too complex and costly for actual instrumentation. Although the instrumentation may be simple for LPG fiber sensors, it is not simple in the sensor fabrication. Hetero-core fiber optic pressure sensor [23] and other macrobend-based sensors [25] have a simple system configuration but their sensor sensitivities may be lower compared with the sensors based on microbending effect.

Microbend optical fiber sensors have differentiating advantages over other optical fiber sensors for the measurement of HR and RR. Firstly, microbend fiber sensors are essential of simple system design, hence favoring a lower system cost and ease of fabrication. Secondly, unlike the conventional fiber sensors that are based on absolute intensity measurement, the current measurement of microbend fiber sensors use relative intensity variation, making it more reliable to its applications. Research on the microbend fiber sensors for vital signs applications was largely overlooked in the past till late 2000 when Grillet and team proposed the use of a new fiber optic microbend sensor for healthcare respiration monitoring [25]. Researches on microbend fiber sensors for vital signs monitoring have been done by some research groups [26–30]. Respiratory monitoring using microbend optical fiber sensor has been investigated in the MRI environment [26]. To validate the potential use of microbend fiber sensor as a medical device, a clinical trial has been studied by simultaneous monitoring the respiration and cardiac activity of patients during sleep [28]. However, most reported publications were for applications in

Corresponding author: Zhihao Chen.

Yi Zhang is with the Photonic Technology Research Center, Quanzhou Normal University, Fujian, China (email: yzhang.cn@outlook.com).

Zhihao Chen is with the School of Physics and Information Engineering and Photonic Technology Research Center, Quanzhou Normal University, Fujian, China (e-mail: zhihaochen@qztc.edu.cn).

Hwan Ing Hee is with KK Women's and Children's Hospital and Duke NUS Medical School, Singapore (email: hee.hwan.ing@singhealth.com.sg).

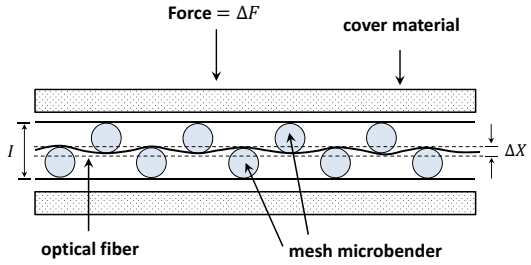

(a) Dual microbenders

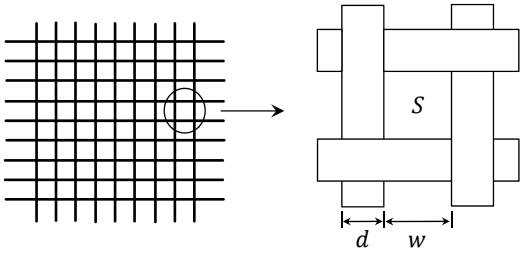

(b) Grid structure

Fig. 1. Schematic of the microbend fiber sensor. S is open area, d is yarn diameter, w is mesh opening

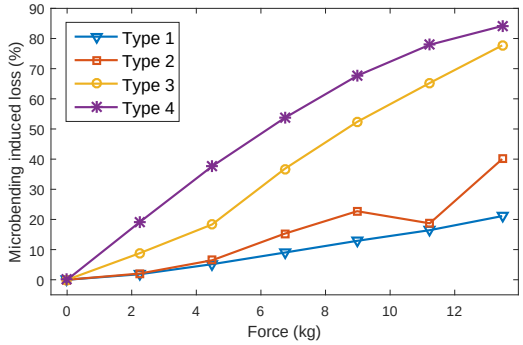

Fig. 2. Microbending induced loss as a function of applied force for different type mesh microbenders

TABLE I
PARAMETERS OF DIFFERENT MESH TYPES

Mesh Type	Material	Mesh opening w (mm)	yarn diameter d (mm)
Type 1	Propyltex	0.420	0.300
Type 2	Propyltex	0.405	0.230
Type 3	Propyltex	0.710	0.440
Type 4	Petex	0.350	0.250

the adult population. Few works were carried out on surgical patients and pediatric patients. There is little data regarding the usability of such a microbend fiber sensor in the infant subset of the pediatric population whose ages ranged from one month to 12 months old.

Algorithms that work well in adult population may not be well applied in infant population as vital parameters such as body weight and vital signs differ vastly between the two population groups including the different sites of measurement [31]. Data from National Center for Health Statistics (Centers for Disease Control and Prevention) reported the 50th percentile weight for a newborn, 12 months old infant and a 20 years old adult to be 3.4-3.8 kg, 9.5-10.4 kg and 58.0-70.5 kg respectively, depending on the gender [32–35]. The mean physiological range of HR for a term neonate, 12 months old and a person above 17-year-old are 110-170 beats per minute (bpm), 85-150 bpm and 60-120 bpm, respectively [36]. While the RR range from 25-60 respirations per minute (rpm), 20-40 rpm and 14-26 rpm are for a term neonate, 12 months old and a person above 17 year old, respectively [36]. Within the infant population from 1 to 12 months, the physiological vital signs change significantly during the first year of life. This within-group variability in vital statistics in the infant population further increases the challenge of clinical applications of the microbend fiber sensor.

To meet the clinical demand of infants (1 month to 12 months old), we have designed and optimized a sensitive microbend optical fiber sensor for perioperative vital signs monitoring for use in the infant subset of the pediatric population. The proposed low-cost device is cable-less and is free from direct contact with skin and electromagnetic interference. In this paper, we design a novel microbend fiber sensor with mesh microbenders to evaluate the feasibility of the microbend optic sensor device in monitoring the HR and RR of infants by comparing the data obtained from the sensor device with that derived from current standard physiological monitoring used in medical settings. Compared with our previous works [26–28], we find right mesh types in a sandwich structure of the microbend optical fiber sensor to meet the phase matching condition so that the microbend loss can be sharply peaked where the conventional multimode fiber is used. Besides, we consider the observations in both time domain and frequency domain, such as harmonic signals for noise removal, to ensure the reliability of the measured HR and RR. Our results show good agreement in HR and RR between our device and the standard physiological monitoring when the patients didn't move in the operation bed. Our new microbend fiber optic sensor is a potential solution for the measurement of HR and RR for perioperative use and in critically ill infants.

II. Device Structure and Working Principles

Fig. 1(a) shows the proposed microbend fiber sensor where a section of graded multimode optical fiber is clamped between a pair of microbenders. Fig. 1(b) is the grid structure of the mesh where S is the open area, d is the yarn diameter and w is the mesh opening. According to the microbending fiber optic theory, the sinusoidal amplitude of the clamped graded multimode optical fiber fluctuates along with the body vibrations as the displacement between two microbenders changes. These vibrations include heart beat, respiratory movements and other vibrations, e.g., body movement. The transmission coefficient T for light propagating in the bent graded multimode fiber is modulated with the body vibrations or body movement. Some light is lost from the fiber core through coupling between guided modes and radiation modes. HR and RR could be

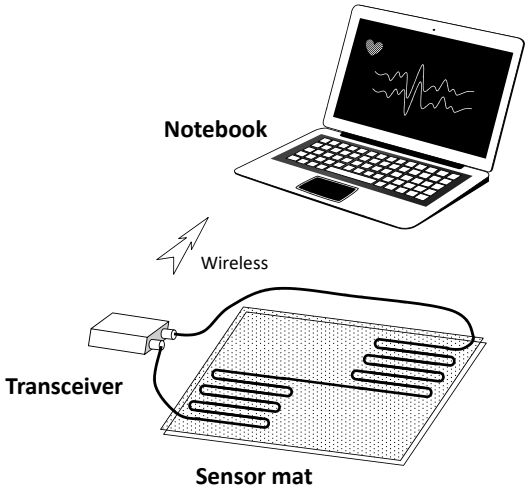

Fig. 3. Instrumentation system

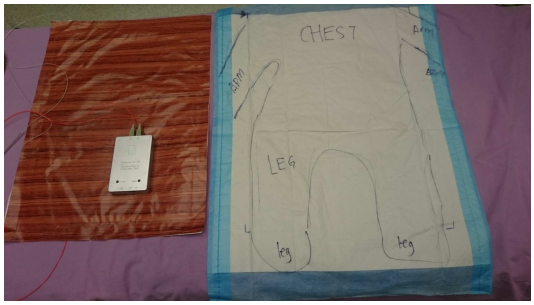

Fig. 4. Sensor mat and position in the operating bed

obtained by demodulating the output signals. The transmission coefficient T is given by [37]

$$\Delta T = (\frac{\Delta T}{\Delta X})\Delta F(k_f + \frac{AY}{I})^{-1}, \tag{1}$$

where ΔF is the force applied to the microbending fiber, ΔX is the displacement of the amplitude of the fiber deformation X, A is the cross-sectional area, Y is the Young's modulus and I is the length of the separation of the two microbenders. The force constant of the microbending fiber, denoted by k_f, can be approximately given by

$$k_f = \frac{\Lambda^3}{3\pi NYD^4}, \tag{2}$$

where D is the diameter of the fiber and N is the number of the bent interval. The critical mechanical pitch, denoted by Λ, is given by

$$\Lambda = \frac{2\pi an}{NA}, \tag{3}$$

where a is the core radius of the fiber, n is the refractive index of the core and NA is the numerical aperture if the fiber. From equations (1)(2)(3), we observe that the sensitivity of the sensor, namely $\Delta T/\Delta F$, depends on a few parameters and has been demonstrated that can be maximized when equation (3) is satisfied. Therefore, the pitch of the microbender Λ is one of the critical parameters in the design.

An experiment, however, is an efficient method to find a right mesh microbender based on the sensitivity $\Delta T/\Delta F$. The results of such an experiment are shown in Fig. 2, where three different types of mesh microbenders are used with the same length of 62.5um multimode fiber as type 1, type 2 and type 3, respectively. Specifically, 100um multimode fiber is demonstrated as type 4 in the loss experiment. The parameters of different mesh types are listed in TABLE I. We observe that type 3 has the higher sensitivity, 5.8%/kg within the 10kg range, than type 1 and type 2. Nevertheless, the best sensitivity, 7.2%/kg within the 10kg range, can be achieved by type 4 among the four types of mesh microbenders. Note that a highly sensitive sensor is preferred for infant application because the body weight of infants is small. We also observe that the sensitivity of Type 4 sensor in terms of slope doesn't have obvious change within the 10kg range as the increase of the force applied to the microbending fiber, that is, the body weight of the infants has little impact to the sensitivity of Type 4. Therefore, we selected type 4 mesh microbenders in our clinical study.

TABLE II
DEMOGRAPHICS OF SUBJECTS INVOLVED IN THE CLINICAL STUDY

Patient No.	Age (month)	Gender	Weight (kg)
#1	11	M	7.6
#2	4	M	5.2
#3	1	F	3.8
#4	8	F	7.8
#5	12	F	8.9
#6	1	M	2.5
#7	12	M	10.2
#8	10	M	3.1
#9	6	M	6.2
#10	12	F	8.6

III. Experimental Results and Discussion

This study was a prospective cross-sectional observational study of infants carried out in the perioperative period in a children's hospital from June 2016 to September 2016. Approval from the Institutional Review Board (IRB 2016/2094) and full parental consent was obtained. Inclusion criteria included infants 1 year and below undergoing surgery and anesthesia in the major operating theater. Exclusion criteria were infants where the supine position was precluded as a result of surgical positioning or abnormality of anatomy and remote anesthesia since supine position is the commonest positioning in the vast majority of surgical procedures, diagnostic procedures as well as resting position during sleep. Ten infants were recruited in the study. Table II shows demographics of the 10 subjects who participated in the observational study. The 9 patients were anesthetized intra-operatively and 1 patient (patient #6) was awake in recovery.

A. Experimental setup

Fig. 3 illustrates a schematic representation of our instrumentation which consists of a sensor mat, a transceiver, and

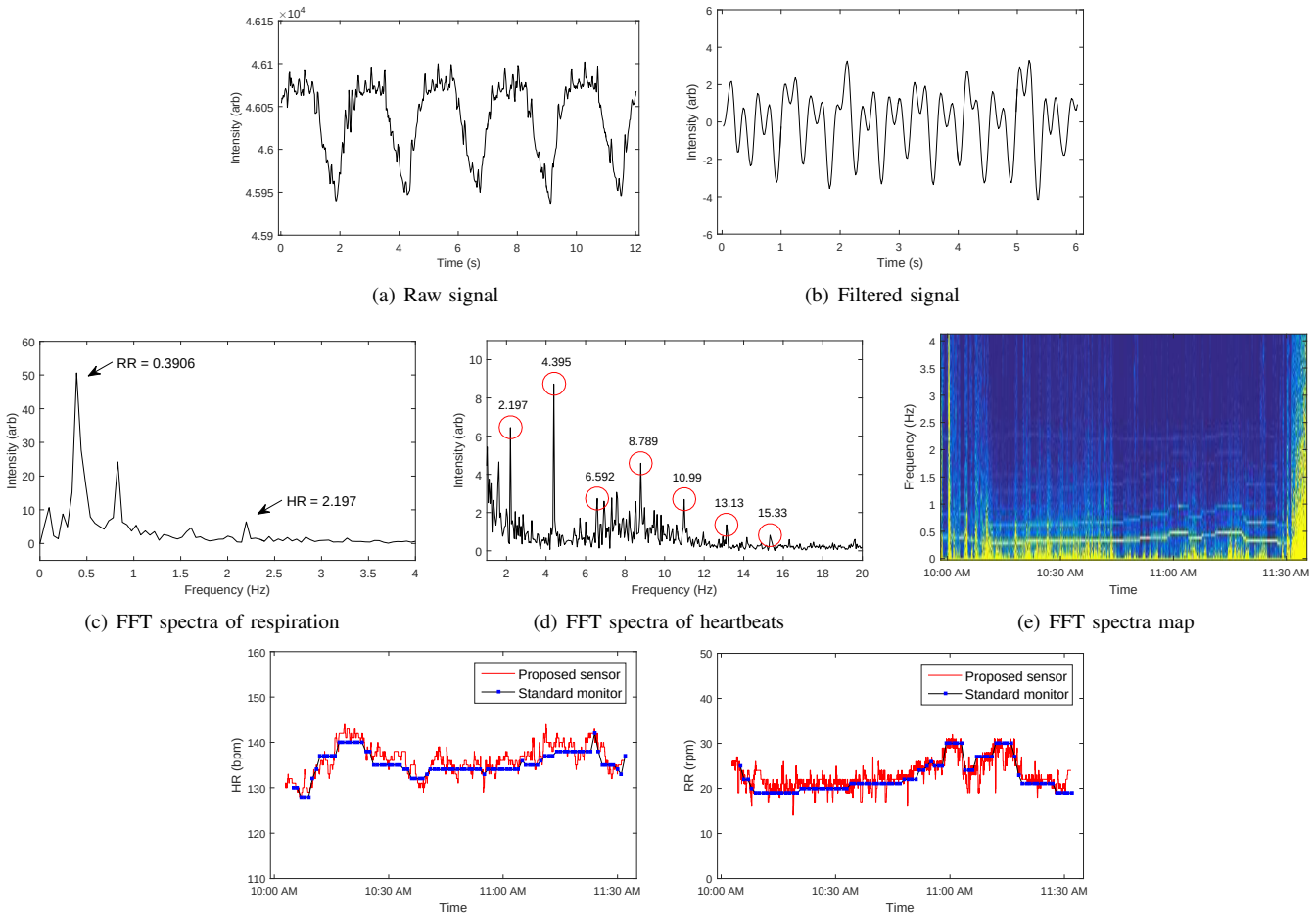

(a) Raw signal (b) Filtered signal

(c) FFT spectra of respiration (d) FFT spectra of heartbeats (e) FFT spectra map

(f) Heart rate (HR) (g) Respiratory rate (RR)

Fig. 5. HR and RR measurement for patient #7

a notebook. The A3 size sensor was covered with wallpaper with a thickness of about 2mm. The essential components of the transceiver consist of a light source at 1310nm, a detector and a microprocessor. The output signal of the transceiver is wirelessly transmitted to a notebook which is sampled at 50Hz. The raw data was saved on the computer. Fig. 4 shows the prototype of the sensor mat used for the clinical study and the position of the patient on the disposable hospital sheet. It should be noted that the sensor device was placed under the infants with the infants in a supine position (lying flat). For infection control purpose, a thin layer of disposable waterproof hospital sheet was placed between all study subjects and the sensor device. The sensor mat is wiped down after each study case.

All standard intraoperative physiological monitoring was applied to all patients as per hospital standard. After administration of general anesthesia, tracheal tubes were inserted and ventilation (rate and volume) was controlled by Draeger ventilator (Draeger Inc, Houston, US) to maintain patients at the normal level of expired end-tidal carbon dioxide (Normocapnia). Standard intraoperative HR monitoring in the operating room was applied with electrocardiography (ECG) using Philips Physiological monitoring (Philips Medical System, MA, US). Standard intraoperative RR monitoring in the operating room included airway spirometry monitoring with Draeger Ventilator and Philips Physiological monitoring.

For the 9 patients under anesthesia, the sensor-derived HR was compared to the HR obtained from ECG with Philips Physiological monitoring. The sensor-derived RR was compared to the RR obtained from spirometry monitoring with Draeger ventilator. For the single awake patient (patient #6), the sensor-derived HR was compared to pulse rate obtained from pulse oximetry (Masimo Corporation, Irvine, US), the sensor-derived respiratory rate was compared to observation and counting of breathing rate by the investigating investigator. At the end of surgery, patients were awakened and allowed to breathe spontaneously before removal of tracheal tubes. These patients were transferred to the recovery room where further observation was carried out. HR monitoring in the recovery was performed with the pulse oximetry and respiration monitoring was monitored by direct observation of breath counts. Clinical data acquisition was performed by the clinical investigator.

B. Measurement

We first discuss how we measure the HR and RR by using the proposed sensor, as illustrated in Fig. 5. Basically, we have the knowledge that the infant's HR generally ranges from 80 to

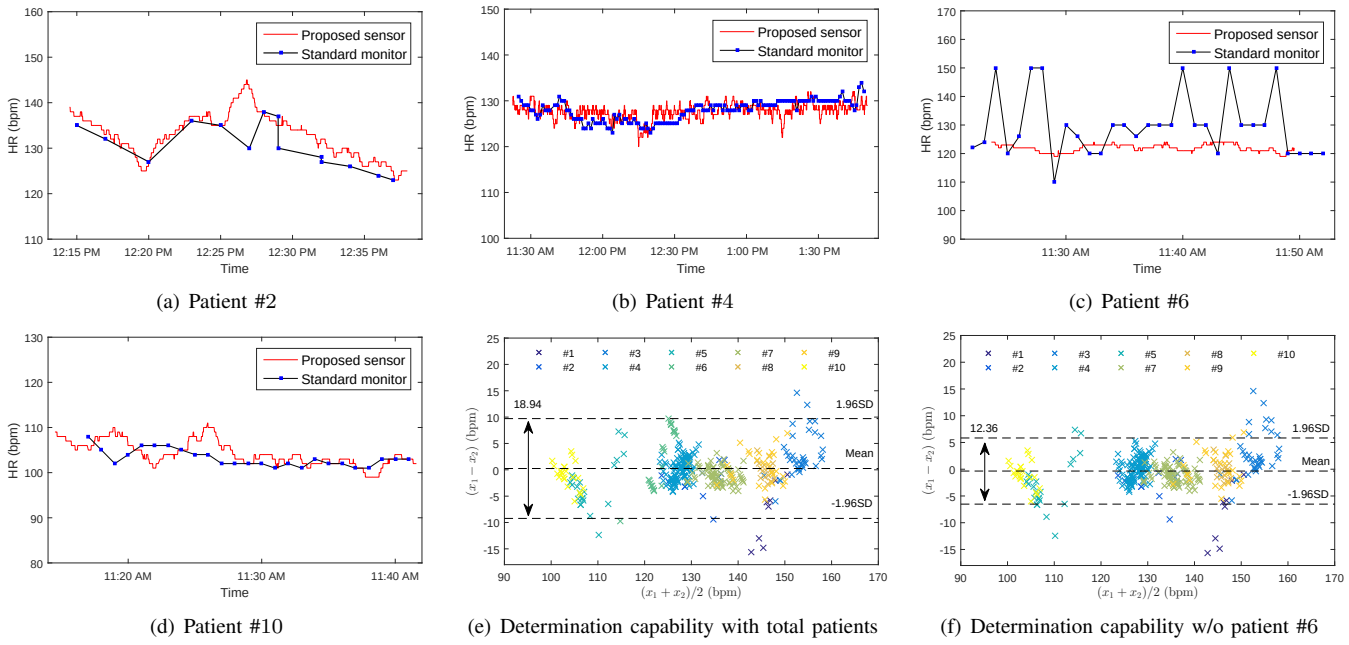

(a) Patient #2 (b) Patient #4 (c) Patient #6

(d) Patient #10 (e) Determination capability with total patients (f) Determination capability w/o patient #6

Fig. 6. Heart rate measurement results

250 bpm (1.33Hz $\sim$ 4.16Hz) and the human RR ranges from 20rpm to 60rpm (0.33Hz $\sim$ 1.00Hz). To ensure the reliability of the measured HR and RR, we combine the observations in both time domain and frequency domain. That is, we first roughly estimate the HR and RR from time domain signal, and then find out the exact HR and RR from the frequency domain signal. In addition, the power of the frequency domain is also used to identify the HR and RR signals. We confirm our measurements when the results derived from the two domains are consistent.

Fig. 5(a) shows a typical raw signal of patient #7 obtained from the proposed sensor, where the respiratory signal and heartbeat signal are clearly seen. The infant was under anesthesia with no gross voluntary body movement. Since the raw signal has about five clear waveforms in continue 12 seconds, the RR of this infant can be estimated as $(60{*}5/12) = 25$ rpm. Furthermore, we observe that there are some lower intensity peaks over the waveform with the near-equal time interval, which are synchronous with the heartbeats of this infant. By operating a signal processing (linear trends removing plus filtering) to the raw signal, heartbeat signal can be retrieved as shown in Fig. 5(b). Therefore, we can roughly calculate the HR as $(60 * 13/6) = 130$ bpm.

Besides, the fast Fourier transformation (FFT) spectra of respiration and heartbeats are shown in Fig. 5(c) and Fig. 5(d), respectively. In Fig. 5(c), the respiratory signal is strong with good signal-to-noise ratio (SNR) detected by the proposed sensor so that the RR can be easily identified as $(60{*}0.3906) \approx 23.5$ rpm. However, the frequency peak of heartbeats in the FFT spectra could not be obviously recognized due to its low intensity. In Fig. 5(d), we find out that the FFT spectra shows not only the fundamental heartbeat frequency (2.197Hz), which can be identified basing on the time domain observation, but also higher order harmonics ($4.395/2 \approx 2.198$Hz, $6.592/3 \approx 2.197$Hz, $8.789/4 \approx 2.197$Hz, $10.99/5 \approx 2.198$Hz, $13.13/6 \approx 2.188$Hz, $15.33/7 \approx 2.190$Hz) of heartbeat signal. The background noise around the fundamental heartbeat frequency is mainly due to the body movement transmitted from surgical manipulation of the patient by the surgeons during the surgery. The feature of the harmonic signals is very useful because it provides more information for the algorithm development for noise removal. Therefore, we confirm the exact frequency of heartbeats as 2.197Hz and measure the HR as $(60 * 2.197) \approx 131.8$ bpm. Furthermore, the FFT spectra map from 10:00AM to 11:30AM is shown in Fig. 5(e), where high brightness indicates high intensity. We observe that the polyline around 0.5Hz is the respiratory signal of patient #7 during the perioperative period.

By adopting both time and frequency domains analysis provided above, the HR and RR of patient #7 can be real-time calculated online in Fig. 5(f) and Fig. 5(g). The blue curve shows the per minute monitoring recorded from the standard physiological hospital monitoring device. The red curve shows the per second measurements derived from the proposed microbend fiber sensor. In Fig. 5(f), the HR range of the infant is between 128 bpm and 145 bpm during the perioperative period. In general, the sensor-derived HR is agreed with the standard monitoring HR. The sensor-derived HR reveals more details of heartbeat variation. In Fig. 5(g), the RR range of the infant is between 18 rpm and 32 rpm. We also observe the sensor-derived RR trace in Fig. 5(g) and the polyline around 0.5Hz in Fig. 5(e) have similar shapes. So far, we have discussed the measurement methods and results by employing the proposed microbend fiber sensor. The experimental results show that the proposed sensor can be regarded as a potential solution that provides continuous measurement of HR and RR for perioperative use and clinical applications.

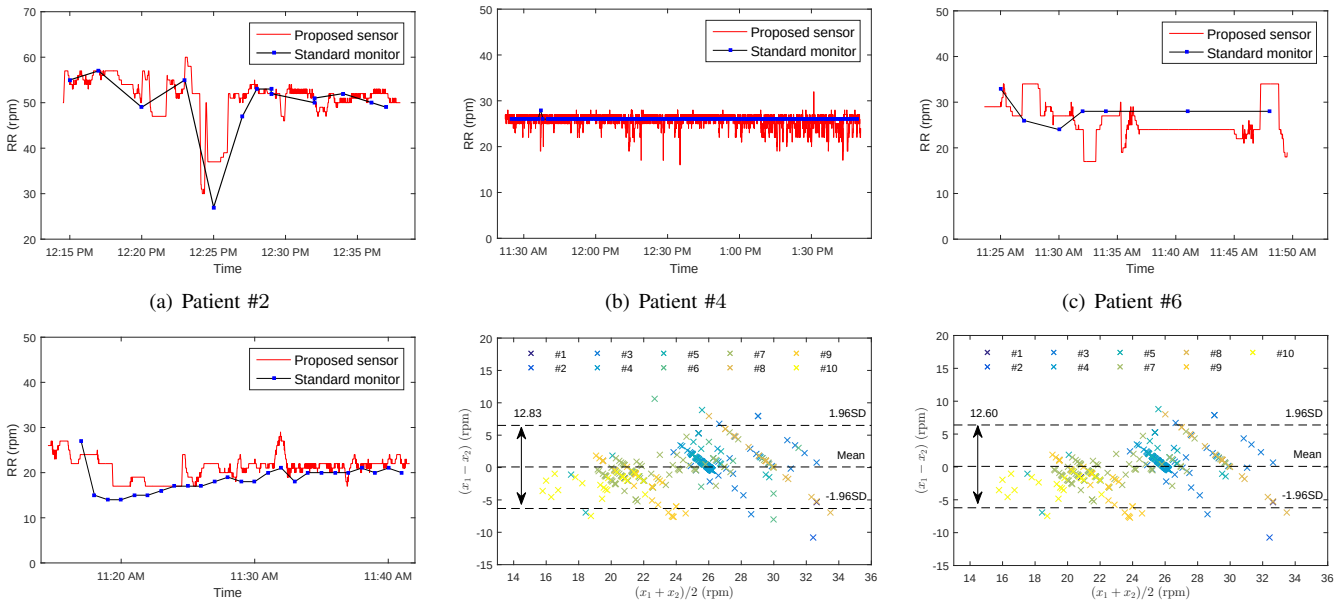

(a) Patient #2 (b) Patient #4 (c) Patient #6

(d) Patient #10 (e) Determination capability with total patients (f) Determination capability w/o patient #6

Fig. 7. Respiratory rate measurement results

TABLE III
SUMMARY OF THE EXPERIMENTAL RESULTS OF THE PROPOSED SENSOR

Patient No.	Acquisition time (h:min)	Heartbeats		Respiration	
		Mean HR (bpm)	SD HR (bpm)	Mean RR (rpm)	SD RR (rpm)
#1	00:21	150.44	5.29	25.63	11.81
#2	00:22	132.72	2.70	50.92	3.50
#3	01:10	151.71	4.09	26.99	3.03
#4	02:24	127.69	1.99	25.56	0.82
#5	00:22	109.73	4.54	24.40	2.95
#6	00:35	122.20	11.52	27.34	5.68
#7	01:29	136.24	1.50	23.00	1.73
#8	00:19	146.17	1.63	28.92	3.76
#9	00:26	144.59	3.09	23.43	3.05
#10	00:22	103.95	2.28	20.64	1.57

C. Heart rate (HR) & Respiratory rate (RR)

During operation, gross movement of patients occurred as a result of surgical manipulation as well as positioning for surgical access. Another source of motion interference arises from the use of forced-air patient warming system. These warming devices are commonly used intra-operatively to keep patients warm. It works by transmitting heat via forced air that is blown through a hose to disperse heated air around the patient's body producing a pulsatile rhythmic vibration of the air current in its immediate environment. Where motion noise occurred, the respiratory signal and heartbeat signal became crumpled, increasing the difficulty and complexity for an algorithm to extract correct signals, especially for heartbeat signal extraction. However, in the absence of gross movements, the signals were clean and accurate data on HR and RR were measured with the proposed sensor device.

Fig. 6 shows the HR measurement results of the proposed micobend fiber sensor. We can see that the sensor-derived HR of those patients, who were anesthetized and motionless with the reduction in motion noise, is close to the standard monitoring HR, such as patient #2 in Fig. 6(a), patient #4 in Fig. 6(b) and patient #10 in Fig. 6(d). Specifically, patient #6 was awake after surgery in the recovery and his voluntary movement resulted in motion noise picked up by the proposed sensor. As shown in Fig. 6(c), the sensor-derived HR fails to respond to the heartbeat variation of patient #6 compared with the conventional pulse oximetry. That is to say, the proposed sensor is suitable to the clinical condition that the patients didn't move in the operation bed. Furthermore, we use the Bland-Altman method [18, 38] in order to assess the determination capability of the proposed sensor. The differences (measurement error) between the sensor-derived HR and the

standard monitoring HR, $x_1 - x_2$, are plotted against the average, $(x_1 + x_2)/2$, in Fig. 6(e). The SD is calculated as the standard deviation of the measurement error between our device and the standard physiological monitoring. According to [18], if 95% of the results lie within a ± 1.96 SD range, then we can claim that the reproducibility is good. Besides, a narrower limit of agreement (LoA) range indicates a better reproducibility. In Fig. 6(e), we find out that 96.66% of the values of the total patients are scattered within the LoA range for the HR (18.94 bpm) determination. Nevertheless, the LoA range for the HR can be reduced to 12.36 bpm in Fig. 6(f) if patient #6 is not considered.

Fig. 7 shows the RR measurement results of the proposed micobend fiber sensor. It should be noted that the respiration of patient #4 was set and controlled intra-operatively by the ventilator machine. Therefore, the RR of patient #4 becomes fixed as shown in Fig. 7(b). We observe that both anesthetized patients and the single awake patient (patient #6) has a good agreement in RR between the proposed sensor and the standard monitoring. That is to say, the motion noise introduces low interference to the respiratory signal so that the RR still can be measured by the proposed sensor device. In Fig. 7(e), 94.94% of the values of the total patients lie with the LoA range for the RR (12.83 rpm) determination. Without considering patient #6, the LoA range has little change in Fig. 7(f), which means that the measurement of RR is comparatively easier than HR measurement.

The total experimental results of the proposed sensor are summarized in Table III. Note that patient #1 is our first testing subject, few HR and RR were recorded from standard physiological monitoring. Thus the measurement results of patient #1 is not good as we expect that patient #1 has the largest SD RR (11.81 rpm) of total patients although its SD HR (5.29 bpm) is acceptable according to the American National Standard ANSI/AAMI EC13: 2002 [39]. Even the single awake patient (patient #6) has 5.69 rpm SD RR. The measured HR of patient #6 is interfered by his motion noise as we have discussed. For the rest of the patients, the results show good agreement in HR and RR between the proposed sensor and the standard monitoring when signals are relatively clean. The maximum SD of HR of patients is 4.54 bpm and the maximum SD of RR is 3.76 rpm. This work shows that the proposed microbend fiber sensor has a satisfactory accuracy for monitoring purposes and the errors are acceptable for clinical applications. The proposed sensor may be used for dual monitoring of HR and RR for small babies with a body weight as low as 2.4kg and become a potential solution for the measurement of HR and RR in perioperative or critically ill neonates and infants.

IV. Conclusion

We have demonstrated a microbend fiber sensor with mesh microbenders to measure HR and RR simultaneously for infants in the perioperative period. In absence of gross movement and in a non-active resting state, the respiratory and heartbeat signals obtained using the sensor device were clean with accurate measurement of HR and RR. Measurement of RR is comparatively easier than HR measurement. This work has shown that the proposed microbend fiber sensor may be used for monitoring the small baby with a body weight as low as 2.5kg and has a potential for health monitoring in the home environment. In clinical settings, potential perioperative use of minimally intrusive monitoring of HR and RR includes postoperative monitoring of newborn and preterm infant. These infants are especially susceptible to episodes of apnea, hypoventilation and bradycardia after general anaesthesia in the immediate postoperative period. In the intraoperative period, the contactless nature of the sensor mat avoids tactile stimulation of traditional monitoring, facilitating a quiescent state for surgery such as neonatal herniotomy to be performed under regional anaesthesia. In the situation where conventional adhesive stick-on monitoring is not amenable, such as in pediatric burn, a common and major injury mechanism in children, contactless monitoring may be a potential alternative during surgery. We recognize that only supine position included in the study is a potential limitation and future study can be undertaken to demonstrate the utility in other positions such as in the lateral and prone positions. Moreover, to overcome motion artifact and expand its application fields, we consider integrating the fiber accelerometer into the current sensor for motion noise elimination.

Acknowledgment

The authors would like to thank Soon Huat Ng, Ju Teng Teo, Xiufeng Yang and Dier Wang for their contributions to our previous work in clinical study [40]. Soon Huat Ng, Ju Teng Teo and Xiufeng Yang are the with Institute for Infocomm Research, Singapore. Dier Wang is with the Nanyang Technological University, Singapore. This work was supported by the fund of Tongjiang Scholar Distinguished Professor and the fund of "Harbour Project" of Quanzhou under Grant 2017ZT013. It is also supported by Fujian Provincial Key Laboratory of Photonics Technology, Key Laboratory of Optoelectronic Science and Technology for Medicine of Ministry of Education, Fujian Normal University, China.

References

[1] J. M. Kortelainen, M. O. Mendez, A. M. Bianchi, M. Matteucci, and S. Cerutti, "Sleep staging based on signals acquired through bed sensor," *IEEE Transactions on Information Technology in Biomedicine*, vol. 14, no. 3, pp. 776–785, 2010.

[2] Y. Chee, J. Han, J. Youn, and K. Park, "Air mattress sensor system with balancing tube for unconstrained measurement of respiration and heart beat movements," *Physiological measurement*, vol. 26, no. 4, p. 413, 2005.

[3] X. Zhu, W. Chen, T. Nemoto, Y. Kanemitsu, K.-i. Kitamura, K.-i. Yamakoshi, and D. Wei, "Real-time monitoring of respiration rhythm and pulse rate during sleep," *IEEE transactions on biomedical engineering*, vol. 53, no. 12, pp. 2553–2563, 2006.

[4] P. De Chazal, C. Heneghan, E. Sheridan, R. Reilly, P. Nolan, and M. O'Malley, "Automated processing of the single-lead electrocardiogram for the detection of obstructive sleep apnoea," *IEEE Transactions on Biomedical Engineering*, vol. 50, no. 6, pp. 686–696, 2003.

[5] G. Matthews, B. Sudduth, and M. Burrow, "A non-contact vital signs monitor," *Critical Reviews™ in Biomedical Engineering*, vol. 28, no. 1&2, 2000.

[6] M. V. Scanlon, "Acoustically monitor physiology during sleep and activity," in *[Engineering in Medicine and Biology, 1999. 21st Annual Conference and the 1999 Annual Fall Meetring of the Biomedical Engineering Society] BMES/EMBS Conference, 1999. Proceedings of the First Joint*, vol. 2. IEEE, 1999, pp. 787–vol.

[7] O. T. Inan, D. Park, L. Giovangrandi, and G. T. Kovacs, "Noninvasive measurement of physiological signals on a modified home bathroom scale," *IEEE Transactions on Biomedical Engineering*, vol. 59, no. 8, pp. 2137–2143, 2012.

[8] L.-G. Lindberg, H. Ugnell, and P. Öberg, "Monitoring of respiratory and heart rates using a fibre-optic sensor," *Medical and Biological Engineering and Computing*, vol. 30, no. 5, pp. 533–537, 1992.

[9] S. Šprager and D. Zazula, "Detection of heartbeat and respiration from optical interferometric signal by using wavelet transform," *Computer methods and programs in biomedicine*, vol. 111, no. 1, pp. 41–51, 2013.

[10] F. C. Favero, V. Pruneri, and J. Villatoro, "Microstructured optical fiber interferometric breathing sensor," *Journal of Biomedical Optics*, vol. 17, no. 3, p. 037006, 2012.

[11] W. SpillmanJr, M. Mayer, J. Bennett, J. Gong, K. Meissner, B. Davis, R. Claus, A. MuelenaerJr, and X. Xu, "A 'smart'bed for non-intrusive monitoring of patient physiological factors," *Measurement Science and Technology*, vol. 15, no. 8, p. 1614, 2004.

[12] T. D. Allsop, R. Bhamber, G. D. Lloyd, M. R. Miller, A. Dixon, D. J. Webb, J. D. Ania-Castañon, and I. Bennion, "Respiratory function monitoring using a real-time three-dimensional fiber-optic shaping sensing scheme based upon fiber bragg gratings," *Journal of biomedical optics*, vol. 17, no. 11, p. 117001, 2012.

[13] A. Silva, J. Carmo, P. Mendes, and J. Correia, "Simultaneous cardiac and respiratory frequency measurement based on a single fiber bragg grating sensor," *Measurement Science and Technology*, vol. 22, no. 7, p. 075801, 2011.

[14] D. Tosi, M. Olivero, and G. Perrone, "Low-cost fiber bragg grating vibroacoustic sensor for voice and heartbeat detection," *Applied optics*, vol. 47, no. 28, pp. 5123–5129, 2008.

[15] T. D. Allsop, T. Earthrowl-Gould, D. J. Webb, and I. Bennion, "Embedded progressive-three-layered fiber long-period gratings for respiratory monitoring," *Journal of biomedical optics*, vol. 8, no. 3, pp. 552–559, 2003.

[16] L. Dziuda, F. W. Skibniewski, M. Krej, and J. Lewandowski, "Monitoring respiration and cardiac activity using fiber bragg grating-based sensor," *IEEE Transactions on Biomedical Engineering*, vol. 59, no. 7, pp. 1934–1942, 2012.

[17] L. Dziuda, F. W. Skibniewski, M. Krej, and P. M. Baran, "Fiber bragg grating-based sensor for monitoring respiration and heart activity during magnetic resonance imaging examinations," *Journal of biomedical optics*, vol. 18, no. 5, p. 057006, 2013.

[18] Ł. Dziuda, M. Krej, and F. W. Skibniewski, "Fiber bragg grating strain sensor incorporated to monitor patient vital signs during MRI," *IEEE Sensors Journal*, vol. 13, no. 12, pp. 4986–4991, 2013.

[19] M. D. Petrović, A. Daničić, V. Atanasoski, S. Radosavljević, V. Prodanović, N. Miljković, J. Petrović, D. Petrović, B. Bojović, L. Hadžievski *et al.*, "Fibre-grating sensors for the measurement of physiological pulsations," *Physica Scripta*, vol. 2013, no. T157, p. 014022, 2013.

[20] T. Allsop, G. Lloyd, R. S. Bhamber, L. Hadzievski, M. Halliday, D. J. Webb, and I. Bennion, "Cardiac-induced localized thoracic motion detected by a fiber optic sensing scheme," *Journal of biomedical optics*, vol. 19, no. 11, p. 117006, 2014.

[21] J. Hao, M. Jayachandran, P. L. Kng, S. F. Foo, P. W. A. Aung, and Z. Cai, "Fbg-based smart bed system for healthcare applications," *Frontiers of Optoelectronics in China*, vol. 3, no. 1, pp. 78–83, 2010.

[22] M. Fajkus, J. Nedoma, R. Martinek, V. Vasinek, H. Nazeran, and P. Siska, "A non-invasive multichannel hybrid fiber-optic sensor system for vital sign monitoring," *Sensors*, vol. 17, no. 1, p. 111, 2017.

[23] M. Nishyama, M. Miyamoto, and K. Watanabe, "Respiration and body movement analysis during sleep in bed using heterocore fiber optic pressure sensors without constraint to human activity," *Journal of biomedical optics*, vol. 16, no. 1, p. 017002, 2011.

[24] J. Wo, H. Wang, Q. Sun, P. P. Shum, and D. Liu, "Noninvasive respiration movement sensor based on distributed bragg reflector fiber laser with beat frequency interrogation," *Journal of Biomedical Optics*, vol. 19, no. 1, p. 017003, 2014.

[25] A. Grillet, D. Kinet, J. Witt, M. Schukar, K. Krebber, F. Pirotte, and A. Depré, "Optical fiber sensors embedded into medical textiles for healthcare monitoring," *IEEE Sensors Journal*, vol. 8, no. 7, pp. 1215–1222, 2008.

[26] D. Lau, Z. Chen, J. T. Teo, S. H. Ng, H. Rumpel, Y. Lian, H. Yang, and P. L. Kei, "Intensity-modulated microbend fiber optic sensor for respiratory monitoring and gating during mri," *IEEE Transactions on Biomedical Engineering*, vol. 60, no. 9, pp. 2655–2662, 2013.

[27] Z. Chen, D. Lau, J. T. Teo, S. H. Ng, X. Yang, and P. L. Kei, "Simultaneous measurement of breathing rate and heart rate using a microbend multimode fiber optic sensor," *Journal of biomedical optics*, vol. 19, no. 5, p. 057001, 2014.

[28] Z. Chen, J. T. Teo, S. H. Ng, X. Yang, B. Zhou, Y. Zhang, H. P. Loo, H. Zhang, and M. Thong, "Monitoring respiration and cardiac activity during sleep using microbend fiber sensor: A clinical study and new algorithm." IEEE, 2014, pp. 5377–5380.

[29] X. Yang, Z. Chen, C. S. M. Elvin, L. H. Y. Janice, S. H. Ng, J. T. Teo, and R. Wu, "Textile fiber optic microbend sensor used for heartbeat and respiration monitoring," *IEEE Sensors Journal*, vol. 15, no. 2, pp. 757–761, 2015.

[30] H.-f. Hu, S.-j. Sun, R.-q. Lv, and Y. Zhao, "Design and experiment of an optical fiber micro bend sensor for respiration monitoring," *Sensors and Actuators A: Physical*, vol. 251, pp. 126–133, 2016.

[31] O. T. Inan, P.-F. Migeotte, K.-S. Park, M. Etemadi, K. Tavakolian, R. Casanella, J. M. Zanetti, J. Tank, I. Funtova, G. K. Prisk *et al.*, "Ballistocardiography and seismocardiography: a review of recent advances." *IEEE J. Biomedical and Health Informatics*, vol. 19, no. 4, pp. 1414–1427, 2015.

[32] [Online]. Available: https://www.cdc.gov/growthcharts/data/set1clinical/cj41l017.pdf

[33] [Online]. Available: https://www.cdc.gov/growthcharts/data/set1clinical/cj41l018.pdf

[34] [Online]. Available: https://www.cdc.gov/growthcharts/data/set1clinical/cj41l021.pdf

[35] [Online]. Available: https://www.cdc.gov/growthcharts/data/set2clinical/cj41l072.pdf

[36] "Normal ranges for physiological variables." [Online]. Available: https://www.rch.org.au/clinicalguide/guideline_index/Normal_Ranges_for_Physiological_Variables/

[37] N. Lagakos, J. Cole, and J. A. Bucaro, "Microbend fiber-optic sensor," *Applied optics*, vol. 26, no. 11, pp. 2171–2180, 1987.

[38] J. M. Bland and D. G. Altman, "Measuring agreement in method comparison studies," *Statistical methods in medical research*, vol. 8, no. 2, pp. 135–160, 1999.

[39] Association for the Advancement of Medical Instrumentation and others, "American national standard ansi/aami ec13: 2002: Cardiac monitors, heart rate meters, and alarms," *Virginia: AAMI*, 2002.

[40] Z. Chen, H. I. Hee, S. H. Ng, J. T. Teo, X. Yang, and D. Wang, "Microbend fiber optic sensor for perioperative pediatric vital signs monitoring," in *Optical Fibers and Sensors for Medical Diagnostics and Treatment Applications XVII*, vol. 10058. International Society for Optics and Photonics, 2017, p. 100580L.